Surface plasmon dispersive spectroscopy of thin films at terahertz frequencies

A.K. Nikitin[*1], O.V. Khitrov[1], A.P. Kyrianov[1], B.A. Knyazev[2,3], G.N. Zhizhin[1]

[1]Scientific and Technological Center for Unique Instrumentation of RAS, 117342 Moscow, Russia
[2]Budker Institute of Nuclear Physics, SB RAS, 630090 Novosibirsk, Russia
[3]Novosibirsk State University, Novosibirsk, 630090, Russia

ABSTRACT

A number of surface plasmon (SP) techniques and devices for terahertz (THz) dispersive spectroscopy of thin films have been developed and reviewed. The techniques are based on the strong dependence of SP complex refractive index κ on the transition layer optical constants. Three of the mentioned techniques employ interference in parallel or quasi parallel beams of bulk and (or) surface waves. These three are remarkable for their accuracy and enable investigators to determine both (real and imaginary) parts of κ in one measuring procedure. Some devices implementing the techniques are static and can have measuring time equal to one pulse duration. Besides, two noninterferometric techniques intended for determining only the real part of κ and assuming tunable monochromatic THz sources are described.

Keywords: Surface plasmons, terahertz radiation, dispersive spectroscopy, thin films, transition layers, interference.

1. INTRODUCTION

Dispersive spectroscopy, called sometimes "dispersion" or "dielectric" spectroscopy, establishes the dielectric properties of a medium as a function of frequency, in other words it determines frequency dependences of optical constants (refractive n and absorption k indexes) as a result of amplitude-phase measurements employing a wide-band continuous or tunable monochromatic radiation source[1,2].

A few decades ago a new powerful method for optical study of conducting surfaces was developed. The method is based on generation of surface plasmons (SP), a kind of surface electromagnetic waves, by probing radiation[3]. SP field has its maximum at the sample's surface and decreases exponentially with moving away from it in any of the two directions. This is the main reason why SP characteristics (propagation length L, phase velocity V_{ph}, and penetration depth in air δ) are very sensitive to optical properties of the surface and its transition layer. Having determined the SP complex refractive index $\kappa=\kappa'+i\cdot\kappa''$, employing the measured $L=(2k_o\cdot\kappa'')^{-1}$ and $V_{ph}=C/\kappa'$ (here $k_o=2\pi/\lambda$, λ - wavelength and and C - speed of the radiation in free space), one can calculate two unknown parameters of the surface layer or the optical constants of the metal substrate. Therefore SP are widely used in surface science of metals as well as for their refractometry, bringing good results in the visible and middle infrared (IR) spectral ranges[4,5].

As for the far IR spectral range, specifically for the terahertz (THz) region (frequencies from 0.1 to 10 THz), SP characteristics are very similar to those of a plane wave in air (with refractive index n): the difference $(\kappa'-n)<10^{-4}$, L amounting to several meters, and δ reaching centimeters[6]. Due to these peculiarities, the process of SP excitation at a clear metal surface is rather embarrassing, which results in very low transformation efficiency (from hundreds to thousandths of a percent) of bulk radiation in THz SP. On the other hand, the SP features at THz frequencies stipulate unacceptably low measurement accuracy both for L and V_{ph}.

The situation improves if we cover the sample surface by a dielectric layer that leads to redistribution of the SP field from air into the metal. The layer's presence increases the value of κ′ and decrease that one of L, making measurement accuracies of these quantities tolerable and the SP spectroscopy technique as a whole efficient at THz frequencies[7].

This paper presents results of our investigations on developing THz SP dispersive spectroscopy. Adaptation of the SP spectroscopy technique to THz range is important due to the following reasons: 1) there is no other optical method intended

[*] alnikitin@mail.ru; phone 7 495 333-5081; fax 7 495 434-7500

Laser Applications in Life Sciences, edited by Matti Kinnunen, Risto Myllylä, Proc. of SPIE Vol. 7376, 73760U · © 2010 SPIE · CCC code: 0277-786X/10/$18 · doi: 10.1117/12.882403

for studying films with thickness $d \ll \lambda$ at THz frequencies; 2) reflectometry and ellipsometry practically cannot be used for conducting surfaces and their transition layers spectroscopy due to the very high reflectivity of metals in the far IR.

Depending on the type of measurements, THz SP dispersive spectroscopy methods may be divided into two groups: interferometric and noninterferometric (Fig.1). The methods are considered below following this classification.

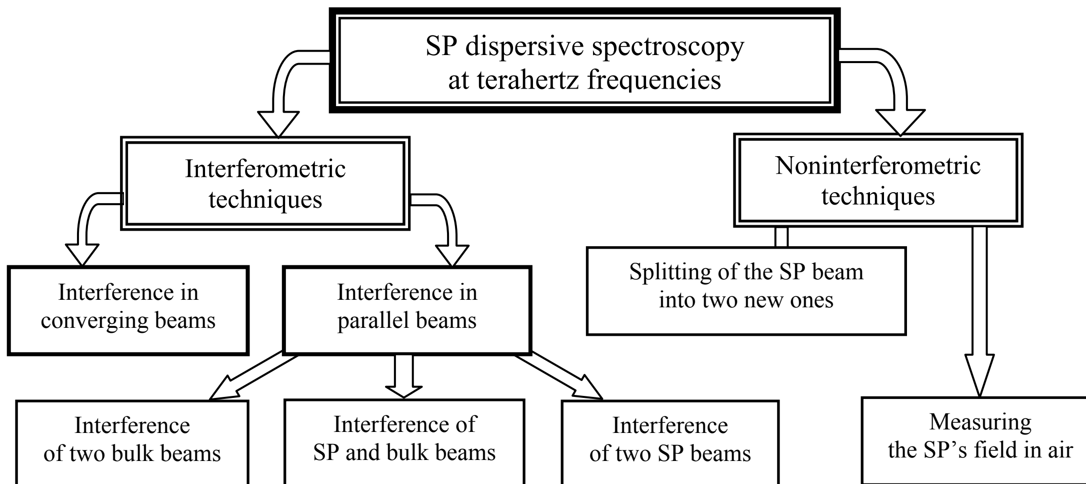

Fig.1. Classification of methods for performing SP dispersive spectroscopy in THz range.

2. INTERFEROMETRIC TECHNIQUES

2.1 Interference SP dispersive spectroscopy in converging bulk beams

The principle idea of interferometric SP spectroscopy described in [4,8] can be realized with a modified Michelson interferometer in which monochromatic radiation in one of the shoulders exists (part of its path) in the form of SP accumulating information about the surface. The information is accumulated in the interference picture formed by two bulk waves: the reference one and the wave produced by the SP due to diffraction at the sample's edge (Fig.2). The interferogram is registered by detector array 4 placed along the axis z at a distance b from the specimen's edge.

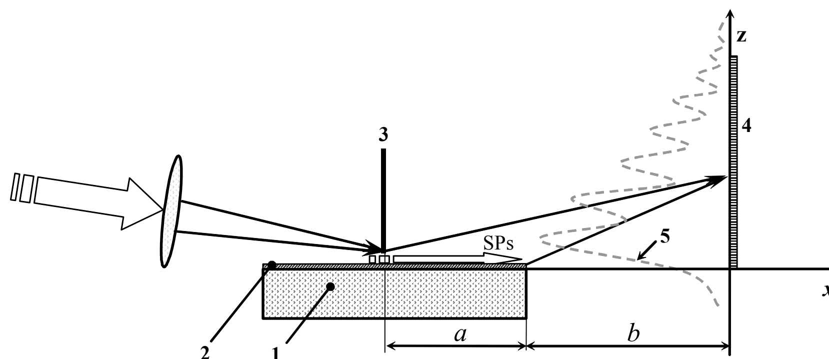

Fig.2. Scheme of the IR SP interferometer [4,8]. Here: 1 – metal sample; 2 – transition layer; 3 – screen with its edge spaced from the specimen surface by a distance of about 10λ; 4 – detector array; 5 – registered interferogram.

However, the accuracy of this method was found to be insufficient as (i) the beams interfere at a large angle, making the period of the pattern comparable with the wavelength; (ii) the pattern depends on the features of the diffraction elements (the screen's edge, transforming the incident radiation in SP and generating the first bulk wave, and the sample's edge, transforming SP into the second bulk wave); and (iii) the wave fronts of the interfering waves significantly differ from planar ones, as a result of which the period and contrast of the interference pattern decrees with an increase in the distance from a sensitive element of array 4 to the specimen's surface.

2.2 Interference SP dispersive spectroscopy in parallel beams

It is quite clear that accuracy of interference measurements is inversely proportional to the convergence angle of the interfering beams. This evidence made us think about a SP interferometer assuming interference in parallel beams. As SP field at THz frequencies extends into air over a distance of several centimeters (reducing its intensity by the $e \approx 2.718$ factor) they can be treated like plane waves in interference and plane mirror reflection processes [9]. Therefore there are three possibilities for realizing SP dispersive spectroscopy in parallel beams: a) interference of two bulk beams; b) interference of two SP beams; c) interference of SP and bulk beams (see Fig.1).

2.3 Interference SP dispersive spectroscopy in parallel bulk beams

This way of performing THz SP dispersive spectroscopy was patented in [10]. The new technique enables one to avoid all the drawbacks inherent to interference in converging bulk beams, but we have to "pay the price" for it by increasing the measurements duration in order to register the detector illumination at a number of distances passed by the SP. Scheme of an interferometer implementing SP dispersive spectroscopy in parallel bulk beams is shown in Fig.3.

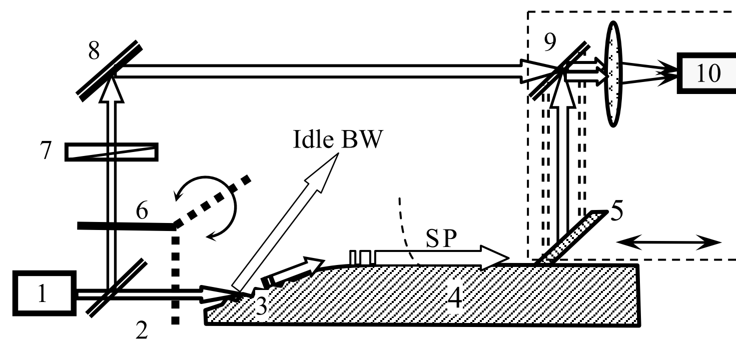

Fig.3. Scheme of a SP interferometer employing interaction of two parallel bulk beams: 1 – frequency tunable source of monochromatic radiation; 2 – beam splitter; 3 - diffractional matching element; 4 – specimen; 5 – moveable mirror abutting against the specimen's surface; 6 – rotatable shutter; 7 – adjustable absorber; 8 – mirror; 9 – beam splitter, conjugated with mirror 5 and photodetector 10 on a mobile platform moving along the specimen's surface.

There are two specific features in this scheme. Firstly, the specimen's surface, guiding SP, has two conjugated facets, joined by a rib rounded off with a radius $R >> \lambda$. One of the facets contains matching element 3 converting radiation of the source in SP, while on the other facet, SP run rather a long distance to mirror 5 transforming them in a bulk wave (BW). This separation of the transforming elements by placing them on different specimen facets is needed to get rid of idle BW originating due to diffraction of the incident radiation on element 3 and was suggested in [11]. Secondly, to realize the reverse transformation process (from SP to BW), plane mirror 5 inclined to the specimen surface is used. Due to inclination the mirror imparts a negative (relative to the SP propagation direction) impact, making the SP wave vector smaller than the BW wave one, that is sufficient for transforming the SP to the BW.

Measurements of the photocurrent I_1 and I_2 should be done at two distances l_1 and l_2 run by the SP and corresponding to known number N of interference maxima. Then values of κ' and κ'' can be calculated using the following formulae:

$$\kappa' = n + \Delta\varphi / (k_o \cdot \Delta l), \quad (1)$$

$$\kappa'' = \frac{ln(I_1/I_2)}{k_o \cdot \Delta l}, \quad (2)$$

here n is refractive index of the radiation in air; $\Delta\varphi = N \cdot \pi$ is the phase difference between SP and the BW stipulated by the inequality of there phase velocities; $\Delta l = l_2 - l_1$.

Substituting so-obtained κ' and κ'' in the SP dispersion equation for a three-layer structure [3, 5], one can determine the transition layer optical constants or the dielectric permittivity of the substrate material (metal).

2.3.1 Interference SP dispersive spectroscopy in parallel surface and bulk beams

It was noted above that SP at THz frequencies can be treated in many respects like plane waves as their field penetrates into air to a distance of several centimeters and their refractive index exceeds that of bulk waves in air only by hundredths or even thousandths of a percent.

On the other hand, as THz SP are mainly excited by means of BW diffraction (either on a grating or on a screen's edge), the problem of phantom BW originating due to the diffraction and propagating along the surface is very urgent. Fields of these BW overlap with the SP field, which embarrasses measurements with THz SP or make them impossible at all. There were rather a number of suggestions how to do away with these phantom BW [11-13].

Taking into consideration these two facts, we elaborated a more simple and effective scheme of a THz SP dispersive spectrometer (Fig.4).

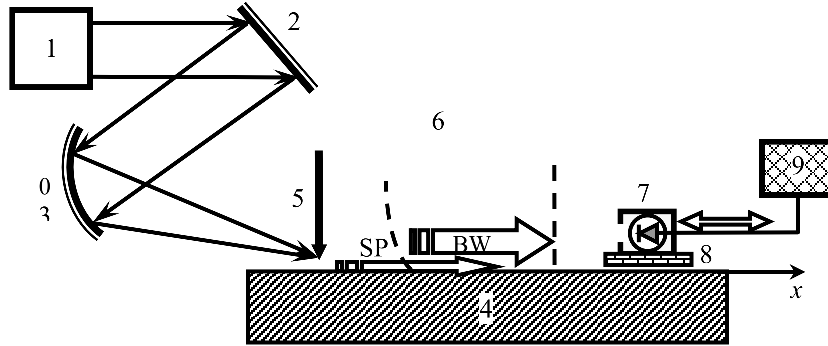

Fig.4. Scheme of the SP spectrometer employing interaction of surface and bulk waves: 1 – tunable source of monochromatic radiation; 2 – mirror; 3 – focusing mirror; 4 – specimen; 5 – screen with its edge spaced from the specimen surface by a distance of about 10λ; 6 – surrounding medium (air); 7 – photo detector placed on the platform 8, moving along the specimen's surface; 9 - data-handling unit.

The spectrometer functions as follows. Using mirrors 2 and 3, radiation of source 1 is directed towards the edge of screen 5, spaced from the specimen plane surface by a controllable distance h. Due to diffraction, the radiation is partially transformed into SP and BW, propagating at various angles from the surface. Among this set of BW there is a beam with a wave vector parallel to the surface and overlapping with the SP field. The BW and SP run along the surface with different phase velocities since κ' is larger than the BW refractive index n. As a result of the Joule loses, the SP intensity decreases exponentially with the absorption factor $\alpha = k_o \cdot \kappa''$. Having covered the same distance x, the BW and SP meet detector 7 and acquire phase incursion differing in value by the magnitude $\Delta\varphi = k_o x \cdot (\kappa' - n)$. Being coherent, the BW and SP interfere and illuminate the detector's sensitive element with the intensity I described by the expression:

$$I(x) = I_1 + I_o \cdot \exp(-\alpha \cdot x) + 2 \cdot \sqrt{I_1 \cdot I_o \cdot \exp(-\alpha \cdot x)} \cdot \cos(\Delta\varphi), \qquad (3)$$

here I_1 is the BW intensity, independent on the distance x; I_o is the SP intensity right under screen 5 when x=0.

The period Λ of the interference pattern (interferogram) registered by the mobile detector 7 is constant. On measuring Λ, one can estimate the SP refractive index value from the evident formula:

$$\kappa' = n + \lambda/\Lambda. \qquad (4)$$

The SP absorption index κ'' can be calculated by putting the SP intensity values measured in two different maxima of the interferogram I_{m1} and I_{m2} in the following formula†:

$$\kappa'' = \frac{2 \cdot ln\left(\frac{\sqrt{I_{m1}} - \sqrt{I_1}}{\sqrt{I_{m2}} - \sqrt{I_1}}\right)}{k_o \cdot (x_2 - x_1)}, \qquad (5)$$

here x_1 and x_2 are the coordinates of corresponding maxima, $x_2 > x_1$.

† Formula derivation is presented in the Appendix.

On putting the found values of κ' and κ'' in the SP dispersion equation for a three-layer structure [3,5], unit 9 computes two parameters of the structure: either the thickness and refractive index of the transition layer or the complex dielectric permittivity of the specimen material $\varepsilon=\varepsilon'+i\cdot\varepsilon''$. Note that the contrast of the interferogram can be controlled by changing the distance h from the screen's edge to the specimen's surface.

To illustrate the technique of THz SP dispersive spectroscopy in parallel surface and bulk beams let us consider the following example. Suppose we have to determine dielectric permittivity of aluminum (*Al*) at λ=100 μm using the method. To reduce L below 30 cm the metal surface is covered with a uniform layer of germanium (*Ge*) 0.7 μm thick. Assume that the screen converting radiation of the source in SP is placed at the distance h ensuring equality $I_1=I_o$, i.e. the intensity of the BW propagating parallel to the surface equals the SP intensity under the screen. The surrounding medium is air (n=1.0002726).

The calculated dependence $I(x)$ for the interferogram in this case is depicted in Fig.5. We carried out the calculations using the Drude model for dielectric permittivity of metals, assigning that the frequencies of plasma ν_p and free electron collision ν_τ for *Al* are equal to 660 cm^{-1} and 119000 cm^{-1}, accordingly[14].

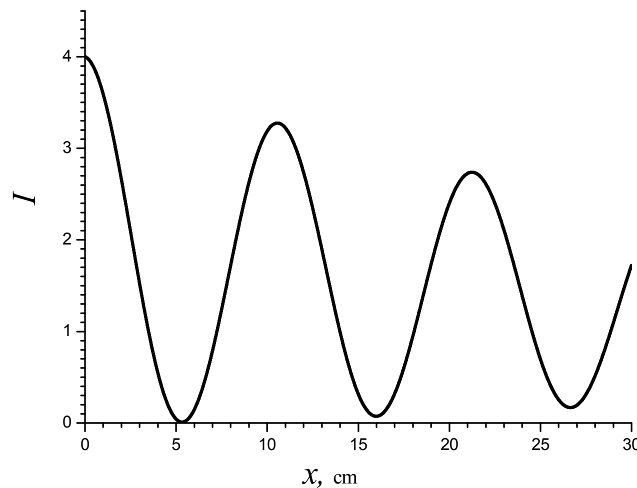

Fig.5. Interferogram calculated for the structure "*Al* –*Ge* layer 0.7 μm thick - air" at λ=100 μm.

Having registered such an interferogram by moving detector 7, one can determine both κ' and κ''. For example, from the graph presented it follows that: 1) the interferogram period Λ=10.675 cm, which according to (4) corresponds to κ'=1.00121; 2) the resulting intensities in the first I_{m1} and the second I_{m2} maxima, reached at the distances x_1=10.565 cm and x_2=21.240 cm, are equal to 3.275 and 2.739 accordingly. Putting the values of I_{m1}, I_{m2}, x_1 and x_2 in (5), we get $\kappa''=6.3\cdot10^{-5}$. At the final stage of the execution procedure we can solve the SP dispersion equation for a three-layer structure relatively to the dielectric permittivity of the metal substrate $\varepsilon=\varepsilon'+i\cdot\varepsilon''$. Thus in the example considered we obtain that *Al* permittivity at λ=100 μm equals to ε_{Al}= -31780+$i\cdot$209745. Having done similar measurements and calculations for other radiation wavelengths one can determine the THz spectra ε' and ε'' of the metal.

Note that there is still no other optical method able to determine these spectra at THz frequencies due to high reflectivity of metals. It is also worth noting that both techniques considered in paragraphs 2.2.1 and 2.2.2 may be used to realize THz SP Fourier-transform spectroscopy in case the incident radiation has a continuous spectrum. We shall study this possibility in the nearest future.

2.3.2 Interference SP dispersive spectroscopy in two parallel surface beams

This way of performing THz SP dispersive spectroscopy was considered in [16] and enables one to reduce the measurement time down to the duration of one source pulse, though such technique is applicable only for monochromatic radiation. The technique implements the concept of asymmetric static interferometry[1] in the planar version, where the interference pattern is formed by surface rather than bulk waves. The pattern formed by the beams

converging at a small angle contains information about both κ' and κ'', which is extracted from the measurement results using mathematical processing.

Fig.6 shows the scheme implementing the technique: 1 - initial SP beam; 2 – sample, guiding the SP; 3 - corner mirror, splitting the initial beam into two coherent beams; 4, 5 - mirrors reflecting the SP beams in the first and second arms of the interferometer; 6 - second corner mirror converging both SP beams; 7 - detector array; 8 - computational device. All mirrors are placed at the surface of sample 2 and oriented perpendicularly to it.

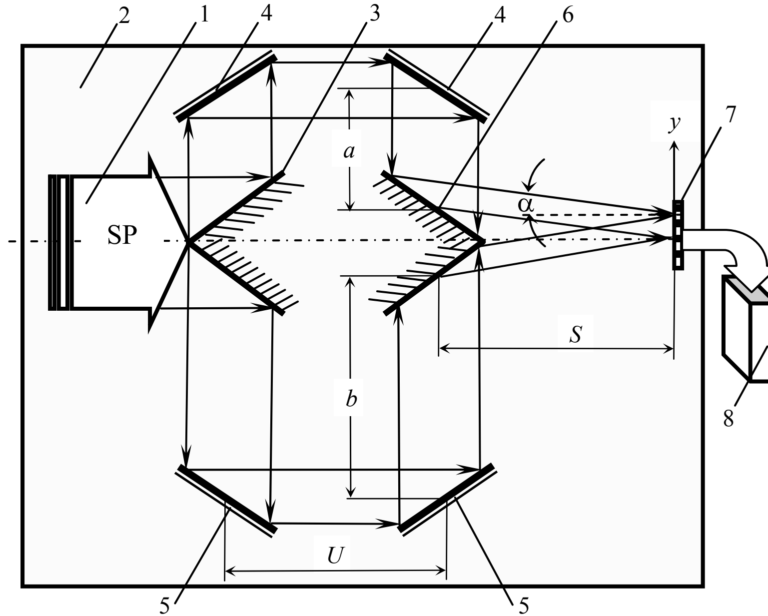

Fig.6. Scheme of the asymmetric static SP interferometer (see notations in the text).

The interferometer works as follows. Initial SP beam 1, guided by the surface of sample 2, reaches corner mirror 3, which splits it in two coherent SP beams propagating perpendicularly to the track of initial beam 1 in opposite directions. The new SP beams reach mirrors 4 and 5, pair wise located at distances a and b from the plane of incidence, reflect from them, and arrive at the adjacent faces of corner mirror 3, oriented so as to make the reflected beams fall on photo detector line 7 at incidence angle α. Having run different distances the SP beams form an interference pattern with the period Λ, which is recorded by line 7. Device 8 uses the electric signals from line 7 and the coordinates of its elements to determine Λ and estimate the luminance in the interference pattern extrema; then, on the basis of these results, it calculates both κ' and κ''.

In accordance with the interference theory [15], the pattern's spatial period Λ relates to κ' as

$$\kappa' = \lambda/[\Lambda\cdot\sin(\alpha)]. \qquad (6)$$

The radiation intensity distribution $I(y)$ on line 7, on the assumption that the interfering SP beams have planar wave fronts, has the following form:

$$I(y) = I_B + I_{Int}, \qquad (7)$$

here I_B is the background component, while I_{Int} is the interference component,

$I_B = I_o\cdot D\cdot\exp[-2k_o\cdot\kappa''(U+S/\cos\alpha)]\cdot\{\exp[(-2k_o\kappa''\cdot(2a+y\cdot\sin\alpha)]+\exp[-2k_o\cdot\kappa''\cdot(2b-y\cdot\sin\alpha)]\}$;

$I_{Int} = I_o\cdot D\cdot\exp[-2k_o\kappa''(U+S/\cos\alpha)]\cdot\exp[-2k_o\kappa''(a+b)]\cdot\cos[2k_o\kappa'\cdot(b-a+y\cdot\sin\alpha)]$;

D is the dynamic (voltage–power) sensitivity of the photo detectors;

$y = 0$ is the coordinate of the center of line 7;

I_o is the initial beam intensity in the face plane of corner mirror 3;

U is the distance between the centers of the beams reflected by mirrors 4 and 5;

S is the distance between the centers of the beams reflected by corner mirror 6 and line 7;
a and b are the half-distances passed by the beams in the directions perpendicular to the initial beam in the first and second interferometer arms;
α is the angle between any interfering beam and the initial beam.

Having measured the interference pattern intensity at points with known coordinates y, one can calculate (solving numerically Eq. (7)) the imaginary part κ'' of the SP refractive index.

Note that successful operation of the interferometer implementing the proposed method implies planar wave fronts of the interfering surface waves; this circumstance simplifies treatment of the measurement results. The condition is reliably satisfied in the direction perpendicular to the sample surface, as the vertical size of the photo detectors is much smaller then the penetration depth of THz SP field in air. The SP wave front in the sample's plane is linear and oriented perpendicularly to the SP propagation direction, as the angular diffraction beam broadening (λ/ω) is small (about 10^{-3} rad) due to the fact that the transverse beam size ω is many times larger than λ [15].

Thus, the transition from the interferometry of bulk waves to the interferometry of surface waves and application of the concept of asymmetric interferometry in this technique make it possible to reduce the measurement time down to the duration of one source pulse.

3. NONINTERFEROMETRIC TECHNIQUES

3.1 SP dispersive spectroscopy by splitting the SP beam into two SP beams

This technique of THz SP dispersive spectroscopy is based on the idea that SP characteristics described by their complex refractive index $\kappa=\kappa'+i\cdot\kappa''$ strongly depend on the presence and parameters of a layer covering the surface[7]. It was stated [17] that as the layer thickness d increases the SP refractive index κ' increases monotonically until it reaches its value for the interface "metal – layer material". As for SP absorption (characterized by κ'') it is almost linearly proportional to d up to the critical value $d_c = \lambda/[4\cdot\sqrt{n_l - 1}]$ (here n_l is the refractive index of "cladding layer"), reaches its maximum at $d = d_c$ and decreases to the value of SP absorption at the interface "metal – layer material" as d trends to infinity.

Transition layers usually have thickness d much smaller than $d_c \approx \lambda$. But still a transition layer makes the THz SP refractive index κ' noticeably exceeding unity, while it reduces the SP propagation length L to the order of centimeters or even tens of centimeters, which is quite sufficient for measuring L with acceptable accuracy using the fool-proof two-prism technique[3,4]. A substantial excess of κ' over unity (the approximate refractive index of air) makes it possible to determine magnitude of κ', employing a dispersive element like a diffractional grating.

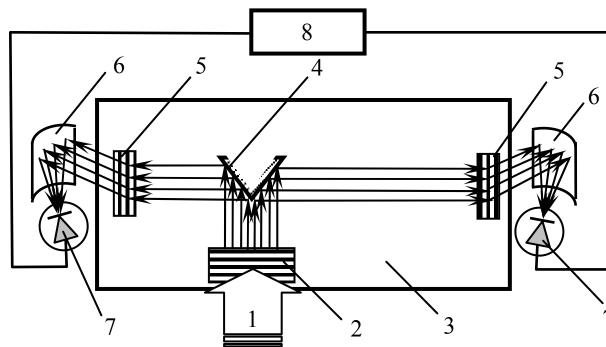

Fig.7. Scheme (view from above) of the noninterferometric SP dispersive spectrometer (notations are in the text).

Their is no problem to measure $\kappa'(\lambda)$ and $L(\lambda)$ dependencies in separate procedures if $0<d<\lambda$. Here we shall consider the scheme of a SP spectrometer able of measuring values of κ' and L simultaneously in one pulse of the radiation source (Fig.7). Suppose the incident radiation 1 is monochromatic. Matching element 2 converts it into a SP beam of width ω guided by a plane surface of specimen 3 supporting a layer of thickness d. On reaching corner mirror 3, the beam is split into two coherent SP beams of equal power propagating in different directions (in particular, oppositely). Having run

different distances along distinct tracks, the new SP beams arrive at identical diffractional gratings 5 with the period Λ and are transformed into bulk waves (BW) propagating in air under the angle φ respective to the SP refractive index κ':

$$n \cdot \sin(\varphi) = \kappa' + \lambda/\Lambda. \tag{8}$$

The radiated BW are focused by cylindrical mirrors 6 and arrive at detectors 7 spaced by the distance y from the plane containing the specimen surface. Thus from eq.(8) data handling unit 8 can calculate κ' provided n, λ and Λ are known and φ (or y) is measured. Comparing the signals I_1 and I_2 from detectors 7, unit 8 can also estimate κ''[3,4]:

$$\kappa'' = \frac{\lambda}{4\pi \cdot L} = \frac{\lambda \cdot ln(I_1/I_2)}{2\pi \cdot \Delta\ell}, \tag{9}$$

here $\Delta\ell$ is the difference of the distances run by the SP beams from mirror 4 to gratings 5.

If the incident radiation is heterogeneous, it should be focused in order to provide the matching condition for each its component. Moreover, instead of single detectors 7 arrays of such detectors disposed normally to the specimen surface should be used. In this case the same radiation components will arrive at different detectors of the arrays in pair wise manner. Coordinates y or numbers of the array detectors will provide information about the angles φ of the components, while currents generated by the detectors will insure determination of L for each component.

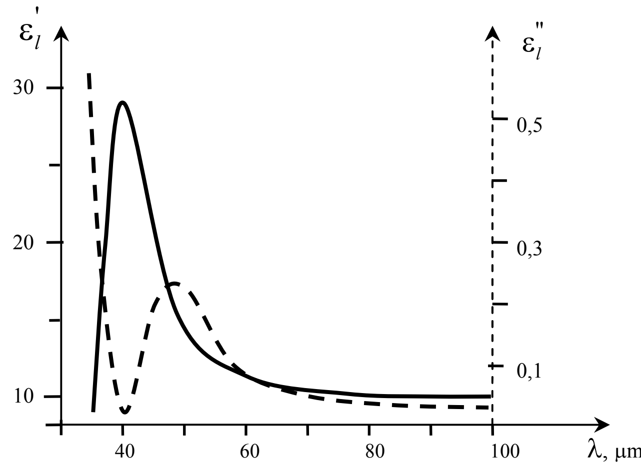

Fig.8. Spectrum of the *ZnS* layer dielectric permittivity $\varepsilon_l = \varepsilon_l' + i \cdot \varepsilon_l''$ (ε_l' - solid line, ε_l'' - dashed line) obtained by the noninterferometric SP dispersive spectrometer utilizing splitting of the initial SP beam into two new ones.

To illustrate the capability of the technique let us consider an example of determining the dielectric permittivity spectrum for zinc sulfide (*ZnS*) layer (thickness d=0.5 μm) deposited on a plane gold surface in the range from 36 μm to 100 μm. A free electron laser or a synchrotron can be used as THz radiation source [18,19]. Suppose matching elements 2 and 5 are corrugation gratings with a period of 300 μm and amplitude of 75 μm. Let us assume that the distance from mirror 4 to left output grating 5 is 5 cm, while the space from the right one is 10 cm. 3.0 cm arrays with 25 μm pixels and placed at 3.0 cm from gratings 2 and 5 will suit as detectors. The environment is air. The Drude model is used for calculating the *Au* dielectric permittivity $\varepsilon = \varepsilon' + i \cdot \varepsilon''$ in assumption that the frequencies of plasma ν_p and free-electron collisions ν_τ are equal to 215 cm^{-1} and 72800 cm^{-1}, accordingly[14]. Assume we have measured the dependencies $\varphi(\lambda)$ and $L(\lambda)$, establishing that φ and L vary from 41°52′ to 62°05′ and from 58.6 mm to 238 mm for λ=36 μm and 100 μm, respectively. Then using (8) and (9) we can calculate the dependencies of $\kappa'(\lambda)$ and $\kappa''(\lambda)$, which will vary in the example at hand from 1.00073 to 1.00368 and $4.9 \cdot 10^{-5}$ до $3.35 \cdot 10^{-4}$, correspondingly. Putting the so-obtained dependencies $\varepsilon(\lambda)$, $\kappa'(\lambda)$ and $\kappa''(\lambda)$ in the SP dispersion equation for a three-layer structure and taking into account the value of d, we can get the spectrum of the *ZnS* layer dielectric permittivity $\varepsilon_l = \varepsilon_l' + i \cdot \varepsilon_l''$ in the frequency range considered (Fig.8).

3.2 SP dispersive spectroscopy employing measurements of the SP field in air

Recently we have found one more way to determine the THz SP complex refractive index. This method involves measurements of the SP propagation length L and the field penetration depth δ into air. The technique is based on two

plain facts: 1) at THz frequencies the magnitude of δ amounts up to centimeters and can be measured easily; 2) the value of δ depends on κ: $\delta = \left[\mathrm{Re}\left(k_2\right)\right]^{-1}$, here $k_2 = k_o \cdot \sqrt{\kappa^2 - n^2}$, n is the refractive index of air. With regard to $L=(2k_o\cdot\kappa'')^{-1}$, one can solve the set of these equations relatively to κ′ and obtain the following formula‡:

$$\kappa' = \frac{1}{k_o} \cdot \sqrt{\frac{1 + k_o^2 \delta^2 \cdot \left[\left(\kappa'\right)^2 + n^2\right]}{1 + k_o^2 \delta^2 \cdot \left(\kappa''\right)^2}} . \tag{10}$$

Fig.9 sketches a device implementing this technique. Monochromatic radiation is incident on matching element 1 located on the surface of specimen 2. Indication and probing of the SP field is realized by detector array 3 established normally to the surface and able to move along the SP track. The array is electrically connected to a personal computer (PC) and contains N pixels.

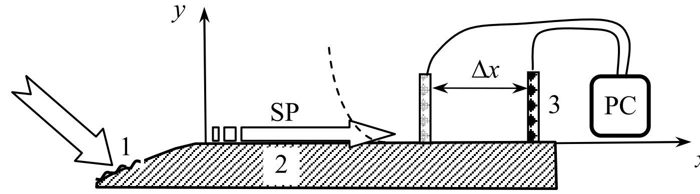

Fig.9. Scheme of the SP dispersive spectrometer employing measurement of SP's field distribution in air (see notations in the text).

Measurements should be done at least at two points of the track spaced from the rounded rib by distances l_1 and l_2. Having integrated signals produced by all pixels of array 3 at each of its two positions, the PC estimates the SP propagation length L using formula (2), thus ensuring κ″ determination. To determine the magnitude of δ the PC has to execute data provided by the array in any of the two positions. Suppose that I_m and I_j are signals produced by the m-th and j-th pixels characterized by coordinates $y_m > y_j$ and spaced by the distance $\Delta y = y_m - y_j$. Then the design formula for δ is the following:

$$\delta = -\frac{\Delta y}{ln\left(I_m / I_j\right)} . \tag{11}$$

Putting the determined values of L and δ in (10), the PC calculates κ′ and finally finds the required values of the transition layer dielectric permittivity $\varepsilon_l = \varepsilon_l^{'} + i \cdot \varepsilon_l^{''}$ at the operation frequency. Combined results of subsequent measurements and calculations at other frequencies, similar to the described above, will represent the required spectra of ε_l.

We should note that there is no need for a real detector array in the considered device. In an extreme situation, the "array" can represent itself two detectors fixed on a line support and separated from each other by a distance Δy comparable with δ.

4. CONCLUSION

A number of techniques and devices employing surface plasmons (SP) for dispersive (dielectric) spectroscopy of thin films deposited on a metal substrate at terahertz (THz) frequencies have been developed and reviewed. These techniques enable scientists to determine spectra of both parts of the transition layer complex dielectric permittivity, which is nowadays impossible to do by any other method in the THz range.

The techniques are based on the strong dependence of the SP complex refractive index κ on the transition layer parameters. It is rather a routine task to measure the SP propagation length related to the imaginary part of κ. But measurements of the real part of κ represent themselves a problem that was resolved earlier exclusively in the interferometric way by using interference of two converging bulk waves one of which had been produced by the SP.

‡ Formula derivation is presented in the Appendix.

We have developed three techniques employing interference in parallel or quasi parallel beams of bulk and (or) surface waves. These techniques are more precise and enable investigators to determine both parts of κ in one measuring procedure. Some of the devices implementing the methods are static and require time equal to one pulse duration.

Besides, two noninterferometric techniques for determining the real part of κ are described and numerically illustrated. These techniques do not require such accurate measurements as the interferometric ones but can be used only when tunable monochromatic THz radiation is employed.

ACKNOWLEDGMENTS

Authors acknowledge the financial support of Russian state contracts P1132 (fulfilled within the Federal Special Program "Scientific, research and educational staff of innovation Russia"), and 02.740.11.0556, as well as the Integration Grant number 89 of the Siberian Branch of the Russian Academy of Science.

REFERENCES

1. Birch, J. R. and Parker, T. J., ″Dispersive Fourier Transform Spectroscopy″, Infr. & Millim. Waves, 2, 137–271 (1977).
2. Volkov, A. A. and Prokhorov, A. S., ″Broadband Dielectric Spectroscopy of Solids″, Radiophysics & Quantum Electronics, 46(8-9), 657-665 (2003).
3. [Surface polaritons. Surface electromagnetic waves at surfaces and interfaces]. Eds. by V.M. Agranovich and D.L. Mills, Amsterdam, New-York, Oxford, 587 (1982).
4. Zhizhin, G.N. and Yakovlev, V.A., ″Broad-band spectroscopy of surface electromagnetic waves″, Phys. Reports, 194(5/6), 281-289 (1990).
5. Nikitin, A.K., [Plasmon optometry]. Dr. Sci. Dissertation. Moscow, 270 (2002).
6. Csurgay, A.I. and Porod, W., ″Surface plasmon waves in nanoelectronic circuits″, Int. J. Circuit Theory & Appl., 32, 339-361 (2004).
7. Zhizhin, G.N., Nikitin, A.K., Bogomolov, G.D. et al., ″Absorption of surface plasmons in “metal-cladding layer-air” structure at terahertz frequencies″, Infrared Phys. & Techn., 49(1-2), 108-112 (2006).
8. Zhizhin, G.N., Alieva, E.V., Kuzik, L.A. et al., ″Free-electron laser for infrared SEW characterization of surfaces of conducting and dielectric solids and nm films on them″, Appl. Phys.(A), 67, 667-673 (1998).
9. Bell, R.J., Goben, C.A., Davarpanah, M. et al., ″Two-dimensional optics with surface electromagnetic waves″, Appl. Optics, 14 (6), 1322-1325 (1975).
10. Zhizhin, G.N., Nikitin, A.K., Balashov, A.A., ″Surface plasmon spectrometer for a conducting surface study in terahertz spectral range″, Russia Federation patent on invention No.2318192, Bul.6 (2008).
11. Koteles, E.S., McNeill, W.H., ″Far infrared surface plasmon propagation″, Int. J. Infr. & Millim. Waves, 2(2), 361-371 (1981).
12. Gong, M., Jeon, T.-I, Grischkowsky, D., ″THz surface wave collapse on coated metal surfaces″, Optics Express, 17(19), 17088-17101 (2009).
13. Zhizhin, G.N., Nikitin, A.K., Nikitin, P.A., ″Method for separation of superposed surface and bulk electromagnetic waves of terahertz spectral range″, Russia Federation patent on invention No. 2352969, Bul.11 (2009).
14. Ordal, M.A., Long, L.L., Bell, R.J., et al., ″Optical properties of the metals Al, Co, Cu, Au, Fe, Pb, Ni, Pd, Pt, Ag, Ti and W in the infrared and far infrared″, Appl. Optics 22(7), 1099-1119 (1983).
15. Born, M. and Wolf, E., [Principles of Optics: Electromagnetic Theory of Propagation, Interference, and Diffraction of Light], Oxford: Pergamon (1964).
16. Bogomolov, G. D., Zhizhin G. N., Kiryanov, A. P., Nikitin, A. K., Khitrov, O. V., ″Determination of the refractive index of IR surface plasmons by static asymmetric interferometry″, Bull. Russian Acad. Science: Physics, 73(4), 533–536 (2009).
17. Schlesinger, Z. and Sievers, A.J., ″IR surface-plasmon attenuation coefficients for *Ge*-coated *Ag* and *Au* metals″, Phys. Rev. (B), 26(12), 6444-6454 (1982).
18. Knyazev, B.A., Kulipanov, G.N., Vinokurov, N.A., ″Novosibirsk terahertz free electron laser: instrumentation development and experimental achievements″, Meas. Sci. Technol., 21, 054017 (2010).
19. Schade, U., Ortolani, M., Lee, J., ″THz experiments with coherent synchrotron radiation from BESSY II″, Synchrotron Rad. News 20(5), 17-24 (2007).

APPENDIX

A1. Derivation of the formula (5)

Suppose we have measured intensity I_{m1} and I_{m2} in two maxima of the interference pattern corresponding to distances x_1 and x_2 run by the SP. With regard to the fact that for maxima $\Delta\varphi=2\pi k$ (here k – is an integer) these intensities in accordance with formula (3) may be described as follows:

$$I_{m1} = I_1 + I_{21} + 2\sqrt{I_1 \cdot I_{21}} \quad \text{and} \quad I_{m2} = I_1 + I_{22} + 2\sqrt{I_1 \cdot I_{22}},$$

here I_1 – is intensity of the bulk wave, I_{21} and I_{22} – are intensities of the SP at coordinates x_1 and x_2. Solving these equations relatively I_{21} and I_{22} we get: $I_{21} = \left(\sqrt{I_{m1}} - \sqrt{I_1}\right)^2$ and $I_{22} = \left(\sqrt{I_{m2}} - \sqrt{I_1}\right)^2$. In view of the exponential SP field decay we can express I_{22} through I_{21} on assumption that $x_1 < x_2$: $I_{22} = I_{21}\cdot\exp(-\alpha\cdot\Delta x)$, here $\alpha = k_o\cdot\kappa''$ - is the SP's absorption coefficient, $\Delta x = x_2 - x_1$. Wherefrom it follows that: $\alpha\cdot\Delta x = ln\left(I_{21}/I_{22}\right)$. Substituting the expressions for I_{21}, I_{22} and α in the last equation we get the required formula (5).

A2. Derivation of the formula (10)

According to the of SP's field penetration depth δ definition it is related to $\kappa=\kappa'+i\cdot\kappa''$ as follows: $\delta = \left[\mathrm{Re}\left(k_o\cdot\sqrt{\kappa^2-\varepsilon}\right)\right]^{-1}$, here $\varepsilon=n^2$ – dielectric constant of air. Then $\mathrm{Re}\left(\sqrt{\kappa^2-\varepsilon}\right) = \left(k_o\cdot\delta\right)^{-1} = A$.

Let's introduce designations: $\kappa'=x_1$ and $\kappa''=x_2$. Then the square root may be presented in the following form:

$$\sqrt{\kappa^2-\varepsilon} = \sqrt{\left(x_1^2 - x_2^2 - \varepsilon\right) + i\cdot 2x_1x_2} = \sqrt{\rho}\cdot\exp(i\cdot\varphi/2), \text{ here } \rho=\sqrt{\left(x_1^2-x_2^2-\varepsilon\right)^2 + \left(2x_1x_2\right)^2}.$$

But in accordance with the trigonometric representation of a complex quantity $c=a+ib$ its real part may be presented as:

$$\mathrm{Re}(c) = \sqrt{a^2+b^2}\cdot\cos(\varphi) = \sqrt{a^2+b^2}\cdot\cos\left[arctg\left(b/a\right)\right].$$

In our case: $\mathrm{Re}\left(\sqrt{\kappa^2-\varepsilon}\right) = \mathrm{Re}\left(\sqrt{\left(x_1^2-x_2^2-\varepsilon\right)+i\cdot 2x_1x_2}\right) = \sqrt[4]{\left(x_1^2-x_2^2-\varepsilon\right)^2+\left(2x_1x_2\right)^2}\cdot\cos\left[\frac{1}{2}\cdot arctg\left(\frac{2x_1x_2}{x_1^2-x_2^2-\varepsilon}\right)\right]$.

Taking into account that: $\cos^2 x = \left[1+\cos(2x)\right]/2$, we can present the previous expression in the following form:

$$\mathrm{Re}\left(\sqrt{\kappa^2-\varepsilon}\right) = \sqrt[4]{\left(x_1^2-x_2^2-\varepsilon\right)^2+\left(2x_1x_2\right)^2}\cdot\sqrt{\left[(1+\cos 2y)/2\right]}, \text{ here } y = \frac{1}{2}\cdot arctg\left(\frac{2x_1x_2}{x_1^2-x_2^2-\varepsilon}\right).$$

But there is the well-known relation: $\cos\left[\mathrm{arctg}(z)\right] = \left(\sqrt{1+z^2}\right)^{-1}$. In our case $z = \dfrac{2x_1x_2}{x_1^2-x_2^2-\varepsilon}$.

Using the latter relation and designation for z, one can obtain:

$$\mathrm{Re}\left(\sqrt{\kappa^2-\varepsilon}\right) = \sqrt{\left[\left(x_1^2-x_2^2-\varepsilon+\sqrt{\left(x_1^2-x_2^2-\varepsilon\right)^2+\left(2x_1x_2\right)^2}\right)\Big/2\right]} = A \text{ (here } A \text{ – quantity introduced above).}$$

Solving this equation relatively x_1 one can get the following answer: $x_1 = A\cdot\sqrt{\dfrac{A^2+x_2^2+\varepsilon}{A^2+x_2^2}}$. Finally, on substituting in the last relation designations for $A=\left(k_o\cdot\delta\right)^{-1}$, $x_1=\kappa'$ and $x_2=\kappa''$, we get the required formula (10).